Alexandria Journal of Medicine (2016) 52, 261–268

HOSTED BY

Alexandria University Faculty of Medicine

Alexandria Journal of Medicine

http://www.elsevier.com/locate/ajme

Finite element model to study two dimensional unsteady state calcium distribution in cardiac myocytes

Kunal Pathak [a,*], **Neeru Adlakha** [b]

[a] *Nirma University, Ahmedabad, Gujarat, India*
[b] *SVNIT, Surat, Gujarat, India*

Received 4 May 2015; accepted 20 September 2015
Available online 20 October 2015

KEYWORDS

Cardiac myocytes;
Reaction diffusion equation;
Excess buffer;
Finite element method

Abstract The calcium signaling plays a crucial role in expansion and contraction of cardiac myocytes. This calcium signaling is achieved by calcium diffusion, buffering mechanisms and influx in cardiac myocytes. The various calcium distribution patterns required for achieving calcium signaling in myocytes are still not well understood. In this paper an attempt has been made to develop a model of calcium distribution in myocytes incorporating diffusion of calcium, point source and excess buffer approximation. The model has been developed for a two dimensional unsteady state case. Appropriate boundary conditions and initial condition have been framed. The finite element method has been employed to obtain the solution. The numerical results have been used to study the effect of buffers and source amplitude on calcium distribution in myocytes.

1. Introduction

Heart is responsible for circulation of blood which is essential for life and functioning of different organs in human body. The functioning of heart is achieved through expansion and contraction of cardiac myocytes. This expansion and contraction of myocytes is responsible for pumping of blood from heart to arteries.[1,2] In order to understand the function of heart it is of crucial interest to understand the processes involved in cardiac myocytes. The various processes involved in spatiotemporal calcium dynamics required for the initiation, termination and sustenance of the activity of the cell are not well understood. Thus there is a need to study the calcium dynamics in cardiac myocytes along with its constituent processes.

Chemical reaction and diffusion are central to quantitative computational biology. Ca^{2+} ions diffuse away from the mouth of voltage gated plasma membrane through Ca^{2+} channels into the cytosolic domain.[1] This domain contains Ca^{2+} binding proteins (Troponin-C). By binding and releasing free Ca^{2+}, endogenous Ca^{2+} binding proteins and other "Ca^{2+} buffers" determine the range of action of Ca^{2+} ions that influence the time course of their effect and facilitate clearance of Ca^{2+}.[1,2] The intracellular binding proteins bind with calcium ion which results in the contraction of cardiac myocytes. The separation of bonded proteins from calcium ion

* Corresponding author.
E-mail addresses: kunal.pathak@nirmauni.ac.in (K. Pathak), neeru.adlakha21@gmail.com (N. Adlakha).
Peer review under responsibility of Alexandria University Faculty of Medicine.

http://dx.doi.org/10.1016/j.ajme.2015.09.007

results in the expansion of cardiac myocytes. The balance of calcium ion is maintained by diffusion of calcium, source influx and buffering mechanism.[1,2]

Attempts are reported in the literature for the study of calcium regulation in neuron cell, astrocyte cell, fibroblast cell, oocyte cell, acinar, etc.[3–19] But very few attempts are reported in the literature for the study of calcium dynamics in myocytes.[1,2,20,21] Most of the studies reported on calcium diffusion in myocytes are experimental.[22–24] In the present paper an attempt has been made to propose a model for calcium dynamics in cardiac myocytes in the presence of excess buffers for a two dimensional unsteady state case. The finite element method has been employed to obtain the solution. The effects of the parameters such as source influx and buffers on the calcium distribution in myocytes have been studied with the help of numerical results.

2. Mathematical formulations

By assuming a bimolecular association reaction between Ca^{2+} and buffer, we have[1]

$$Ca^{2+} + B \underset{k^-}{\overset{k^+}{\Longleftrightarrow}} CaB \tag{1}$$

In Eq. (1), B represents free buffer, and CaB represents Ca^{2+} bound buffer. k^+ and k^- are association and dissociation rate constants, respectively. If it is further assumed that the reaction of Ca^{2+} with buffer follows mass action kinetics, then the system of ODEs for the change in concentration of each species is given by[1,2]

$$\frac{\partial[Ca^{2+}]}{\partial t} = R + J \tag{2}$$

$$\frac{\partial[B]}{\partial t} = R \tag{3}$$

$$\frac{\partial[CaB]}{\partial t} = -R \tag{4}$$

where the common reaction term R, is given by

$$R = -k^+[Ca^{2+}][B] + k^-[CaB] \tag{5}$$

and J represents Ca^{2+} influx. Both R and J have units of concentration per unit time. Eqs. (2)–(5) are extended to include multiple buffers and the diffusive movement of free Ca^{2+}, Ca^{2+} bound buffer and Ca^{2+} free buffer. Assuming, Fick's diffusion in a homogeneous, isotropic medium, the system of reaction diffusion equations can be written as[1,2]

$$\frac{\partial[Ca^{2+}]}{\partial t} = D_{Ca}\nabla^2[Ca^{2+}] + \sum_i R_i + J \tag{6}$$

$$\frac{\partial[B_i]}{\partial t} = D_{B_i}\nabla^2[B_i] + R_i \tag{7}$$

$$\frac{\partial[CaB_i]}{\partial t} = D_{CaB_i}\nabla^2[CaB_i] - R_i \tag{8}$$

where the reaction term, R_i is given by

$$R_i = -k_i^+[Ca^{2+}][B_i] + k_i^-[CaB_i] \tag{9}$$

Here i is an index over Ca^{2+} buffers. $D_{Ca}, D_{B_i}, and D_{CaB_i}$ are diffusion coefficients of free Ca^{2+}, bound calcium and free buffer respectively.

Since Ca^{2+} has a molecular weight that is small in comparison with most Ca^{2+} binding species, the diffusion constant of each mobile buffer is not affected by the binding of Ca^{2+} that is $D_{B_i} = D_{CAB_i} = D_i$.[1,2] Substituting this in Eqs. (7) and (8) and on summation it gives

$$\begin{aligned}\frac{\partial[B_i]_T}{\partial t} &= \frac{\partial[CaB_i]}{\partial t} + \frac{\partial[B_i]}{\partial t} \\ &= D_i\nabla^2[CaB_i] + D_i\nabla^2[B_i] \\ &= D_i\nabla^2[B_i]_T\end{aligned} \tag{10}$$

And

$$R_i = -k_i^+[Ca^{2+}][B_i] + k_i^-([B_i]_T - [B_i]) \tag{11}$$

where

$$[B_i]_T = [CaB_i] + [B_i] \tag{12}$$

Thus, $[B_i]_T$, profiles are initially uniform and there are no sources or sinks for Ca^{2+} buffer, and $[B_i]_T$ remains uniform for all times.[1,2] Thus, the following equations can be written for the diffusion of Ca^{2+}:

$$\frac{\partial[Ca^{2+}]}{\partial t} = D_{Ca}\nabla^2[Ca^{2+}] + \sum_i R_i + J \tag{13}$$

$$\frac{\partial[B_i]}{\partial t} = D_i\nabla^2[B_i] + R_i \tag{14}$$

where

$$R_i = -k_i^+[Ca^{2+}][B_i] + k_i^-([B_i]_T - [B_i]) \tag{15}$$

In the excess buffer approximation (EBA), Eqs. (6)–(8) are simplified by assuming that the concentration of free Ca^{2+} buffer $[B_i]$, is high enough such that its loss is negligible. The EBA gets its name because this assumption of the unsaturability of Ca^{2+} buffer is likely to be valid when Ca^{2+} buffer is in excess.[7]

The association and dissociation rate constants for the bimolecular association reaction between Ca^{2+} and buffer can be combined to obtain a dissociation constant, K_i as follows:

$$K_i = k_i^-/k_i^+ \tag{16}$$

This dissociation constant of the buffer has units of μM and is the concentration of Ca^{2+} which is necessary to cause 50% of the buffer to be in Ca^{2+} bound form. To show this consider the steady state of Eqs. (6)–(8) in the absence of influx ($J = 0$). Setting the left hand sides of Eqs. (7) and (8) to zero gives[7]

$$[B_i]_\infty = \frac{K_i[B_i]_T}{K_i + [Ca^{2+}]_\infty} \tag{17}$$

and

$$[CaB_i]_\infty = \frac{[Ca^{2+}]_\infty[B_i]_T}{K_i + [Ca^{2+}]_\infty} \tag{18}$$

where $[Ca^{2+}]_\infty$ is the "background" or ambient free Ca^{2+} concentration. And $[B_i]_\infty$ and $[CaB_i]_\infty$ are the equilibrium concentrations of free and bound buffer with respect to index i. In this expression K_i is the dissociation rate constant of buffer i. Note that higher values for K_i imply that the buffer has a lower affinity for Ca^{2+} and is less easily saturated. In this case, the equation for the diffusion of Ca^{2+} becomes

$$\frac{\partial[Ca^{2+}]}{\partial t} = D_{Ca}\nabla^2[Ca^{2+}] - \sum_i k_i^+[B_i]_\infty([Ca^{2+}] - [Ca^{2+}]_\infty) \tag{19}$$

To complete a reaction–diffusion formulation for the buffered diffusion of Ca^{2+}, a particular geometry of simulation must be specified and Eq. (19) must supplement with boundary conditions. If Ca^{2+} is released from intracellular Ca^{2+} stores deep within a large cell (so that the plasma membrane is far away and does not influence the time course of the event), and the intracellular milieu is homogenous and isotropic, then it has cylindrical symmetry.[1] In this case the evolving profiles of Ca^{2+} and buffer will be a function of r and θ only. For a two dimensional unsteady state case the Eq. (19) in polar cylindrical coordinates in the absence of influx ($J = 0$) is given by

$$\frac{1}{r}\frac{\partial}{\partial r}\left(r\frac{\partial[Ca^{2+}]}{\partial r}\right)+\frac{1}{r^2}\frac{\partial^2[Ca^{2+}]}{\partial\theta^2}-\frac{k^+[B]_\infty}{D_{Ca}}([Ca^{2+}]-[Ca^{2+}]_\infty)=\frac{1}{D_{Ca}}\frac{\partial[Ca^{2+}]}{\partial t} \tag{20}$$

The reasonable boundary condition for this simulation is uniform background Ca^{2+} profile of $[Ca^{2+}]_\infty = 0.1$ μM. It is required that buffer far from the source to remain in equilibrium with Ca^{2+} at all times. Thus the boundary condition on the boundary away from the source is given by[1,2,17]

$$\lim_{r\to\infty,\theta\to 0}[Ca^{2+}]=[Ca^{2+}]_\infty \tag{21}$$

At the source, it is assumed that influx takes place and therefore the boundary condition is expressed as[1,2,17]

$$\lim_{r\to\infty,\theta\to\pi}\left(-2\pi D_{Ca}r\frac{\partial[Ca^{2+}]}{\partial r}\right)=\sigma_{Ca} \tag{22}$$

We define an influx of free Ca^{2+} at the rate σ_{Ca} by Faraday's law, $\sigma_{Ca}=\frac{I_{Ca}}{zF}$ where I_{Ca} is amplitude of elemental Ca^{2+} release, F is Faraday's constant and Z is valence of Ca^{2+}.[1,2,17]

The initial concentration at $t = 0$ s is taken as 0.1 μM. i.e.

$$\lim_{t\to 0}[Ca^{2+}]=0.1\ \mu M \tag{23}$$

Hence, the problem reduces to find the solution of Eq. (20) with respect to the boundary conditions (21) and (22) and initial condition (23). Here, $[Ca^{2+}]_\infty$ is the background calcium concentration, $[B]_\infty$ is the total buffer concentration, and σ_{Ca} represents the flux. $[Ca^{2+}]$ achieves its background concentration 0.1 μM as r tends to ∞ and θ tends to π. But the domain taken here is not infinite but finite one. Here, the distance is taken as required for $[Ca^{2+}]$ to attain background concentration as 7.8 μm for the cardiac myocytes (i.e. radius of the cardiac myocytes).[10] Now the finite element method is employed to solve Eq. (20) with boundary conditions (21) and (22) and initial condition (23).

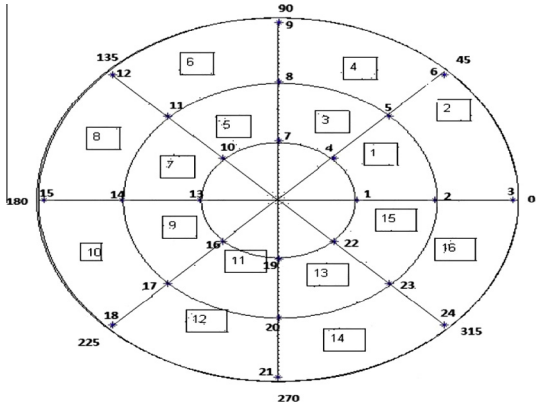

Figure 1 Finite element discretization of circular cell.

Assuming that the cardiac myocytes are of circular shape, it is divided into sixteen coaxial circular elements, as shown in Fig. 1.

Here the number in square represents the number of elements and member without square represents the nodal points where the nodal point (7.8, π) represents point source of calcium. The following table represents the element information (see Table 1).

The discretized variational form of Eq. (20) is given by

$$\begin{aligned}I^{(e)}=&\tfrac{1}{2}\int_{r_i}^{r_j}\int_{\theta_i}^{\theta_j}\left[\left(r\left(\tfrac{\partial y^{(e)}}{\partial r}\right)^2+\tfrac{1}{r}\left(\tfrac{\partial y^{(e)}}{\partial\theta}\right)^2\right)\right]dr\,d\theta\\&+\tfrac{1}{2}\int_{r_i}^{r_j}\int_{\theta_i}^{\theta_j}\left[\tfrac{k^+[B]_\infty}{D_{Ca}}ry^{(e)2}-\tfrac{2k^+[B]_\infty}{D_{Ca}}y_\infty y^{(e)}r\right]dr\,d\theta\\&\tfrac{1}{2}\int_{r_i}^{r_j}\int_{\theta_i}^{\theta_j}\left[\tfrac{r}{D_{Ca}}\tfrac{\partial y^{(e)2}}{\partial t}\right]dr\,d\theta-\int_{\theta_i}^{\theta_j}\left[\tfrac{\sigma_{Ca}}{2\pi D_{Ca}}ry^{(e)}\right]d\theta\end{aligned} \tag{24}$$

Here, 'y' is used in lieu of $[Ca^{2+}]$ for our convenience, $e = 1, 2, \ldots, 16$.

The following bilinear shape function for the calcium concentration within each element has been taken as

$$y^{(e)}=C_1^{(e)}+C_2^{(e)}r+C_3^{(e)}\theta+C_4^{(e)}r\theta \tag{25}$$

In matrix form the Eq. (25) can be written as

$$y^{(e)}=P^TC^{(e)} \tag{26}$$

where

$$P^T=[1\ r\ \theta\ r\theta]\ \text{and}\ C^{(e)}=\begin{bmatrix}C_1^{(e)}\\C_2^{(e)}\\C_3^{(e)}\\C_4^{(e)}\end{bmatrix}$$

Also

$$y_i^{(e)}=C_1^{(e)}+C_2^{(e)}r_i+C_3^{(e)}\theta_i+C_4^{(e)}r_i\theta_i \tag{27}$$

$$y_j^{(e)}=C_1^{(e)}+C_2^{(e)}r_j+C_3^{(e)}\theta_j+C_4^{(e)}r_j\theta_j \tag{28}$$

$$y_k^{(e)}=C_1^{(e)}+C_2^{(e)}r_k+C_3^{(e)}\theta_k+C_4^{(e)}r_k\theta_k \tag{29}$$

$$y_l^{(e)}=C_1^{(e)}+C_2^{(e)}r_l+C_3^{(e)}\theta_l+C_4^{(e)}r_l\theta_l \tag{30}$$

Using Eqs. (27)–(30) we get

$$\bar{y}^{(e)}=P^{(e)}C^{(e)} \tag{31}$$

where

$$P^{(e)}=\begin{bmatrix}1&r_i&\theta_i&r_i\theta_i\\1&r_j&\theta_j&r_j\theta_j\\1&r_k&\theta_k&r_k\theta_k\\1&r_l&\theta_l&r_l\theta_l\end{bmatrix}\quad\text{and}\quad\bar{y}^{(e)}=\begin{bmatrix}y_i^{(e)}\\y_j^{(e)}\\y_k^{(e)}\\y_l^{(e)}\end{bmatrix}$$

From Eqs. (26) and (31) we get

$$y^{(e)}=P^TR^{(e)}\bar{y}^{(e)} \tag{32}$$

where $R^{(e)}=P^{(e)-1}$.

Now the integral given in Eq. (24) can also be written as,

Table 1 Element information.

e	i	j	k	l
1	1	2	4	5
2	2	3	5	6
3	4	5	7	8
4	5	6	8	9
5	7	8	10	11
6	8	9	11	12
7	10	11	13	14
8	11	12	14	15
9	13	14	16	17
10	14	15	17	18
11	16	17	19	20
12	17	18	20	21
13	19	20	22	23
14	20	21	23	24
15	22	23	1	2
16	23	24	2	3

Table 2 Numerical values of biophysical parameters.[10]

R	Radius of the cell	7.8 μm
I_{Ca}	Amplitude of elemental Ca^{2+} release	1 pA
F	Faraday's constant	6500 C/mol
Z	Valence of Ca^{2+} ion	2
D_{Ca}	Diffusion coefficient of free Ca^{2+} in cytosol for Troponin C	780 $\mu m^2/s$
$[B_1]_T$	Total concentration for each Ca^{2+} buffer of Troponin C	70 μM
k^+	Association rate constant for Ca^{2+} binding of Troponin C	39 $\mu M^{-1}\,s^{-1}$
k^-	Dissociation rate constant for Ca^{2+} binding of Troponin C	20 s^{-1}
K	Dissociation constant of Troponin $C = \frac{k_1^-}{k_1^+}$	0.51 μM
$[Ca]_\infty$	Intracellular free Ca^{2+} concentration at rest	0.1 μM

$$
\begin{aligned}
I^{(e)} = & \frac{1}{2}\int_{r_i}^{r_j}\int_{\theta_i}^{\theta_k}\left[r\left(P_r^T R^{(e)}\bar{y}^{(e)}\right)^2+\frac{1}{r}\left(P_\theta^T R^{(e)}\bar{y}^{(e)}\right)^2\right]dr\,d\theta \\
& +\frac{1}{2}\int_{r_i}^{r_j}\int_{\theta_i}^{\theta_k}\left[\frac{k^+[\mathrm{B}]_\infty}{D_{\mathrm{Ca}}}r\left(P^T R^{(e)}\bar{y}^{(e)}\right)^2\right]dr\,d\theta \\
& -\frac{1}{2}\int_{r_i}^{r_j}\int_{\theta_i}^{\theta_k}\left[\frac{2k^+[\mathrm{B}]_\infty}{D_{\mathrm{Ca}}}u_\infty r\left(P^T R^{(e)}\bar{y}^{(e)}\right)\right]dr\,d\theta \\
& \frac{1}{2}\int_{r_i}^{r_j}\int_{\theta_i}^{\theta_k}\left[\frac{r}{D_{\mathrm{Ca}}}\frac{\partial}{\partial t}\left(P^T R^{(e)}\bar{y}^{(e)}\right)^2\right]dr\,d\theta-\int_{\theta_i}^{\theta_k}\left[\frac{\sigma_{\mathrm{Ca}}}{2\pi D_{\mathrm{Ca}}}r\bar{y}^{(e)}\right]d\theta
\end{aligned}
\tag{33}
$$

Now $I^{(e)}$ is minimized with respect to $\bar{y}^{(e)}$, and we have

$$\frac{dI^{(e)}}{d\bar{y}^{(e)}}=0 \tag{34}$$

where

$$\bar{y}^{(e)}=\left[y_i\ y_j\ y_k\ y_l\right]^T, e=(1,2,\ldots,16)$$

and

$$\frac{dI}{d\bar{y}^{(e)}}=\sum_{e=1}^{N}\bar{M}^{(e)}\frac{dI^{(e)}}{d\bar{y}^{(e)}}\bar{M}^{(e)T} \tag{35}$$

$$\bar{M}^{(e)}=\begin{bmatrix}0&0&0&0\\1&0&0&0\\0&1&0&0\\0&0&1&0\\0&0&0&1\\\bullet&\bullet&\bullet&\bullet\\0&0&0&0\end{bmatrix}_{(24\times4)}\begin{matrix}\\(ith\ row)\\(jth row)\\(kth row)\\(lth row)\\\\\end{matrix}\quad\text{and}\quad I=\sum_{e=1}^{16}I^{(e)}$$

This leads to following system of linear algebraic equations:

$$[A]_{(24\times24)}\frac{d}{dt}[\bar{y}]_{(24\times1)}+[B]_{(24\times24)}[\bar{y}]_{(24\times1)}=[C]_{(24\times1)} \tag{36}$$

Here, $\bar{y}=[y_1\quad y_2\ \bullet\ \bullet\ \bullet\ y_{24}]^T$, A and B are system matrices and C is characteristic vector. Crank Nicolson method is employed to solve the system (35).

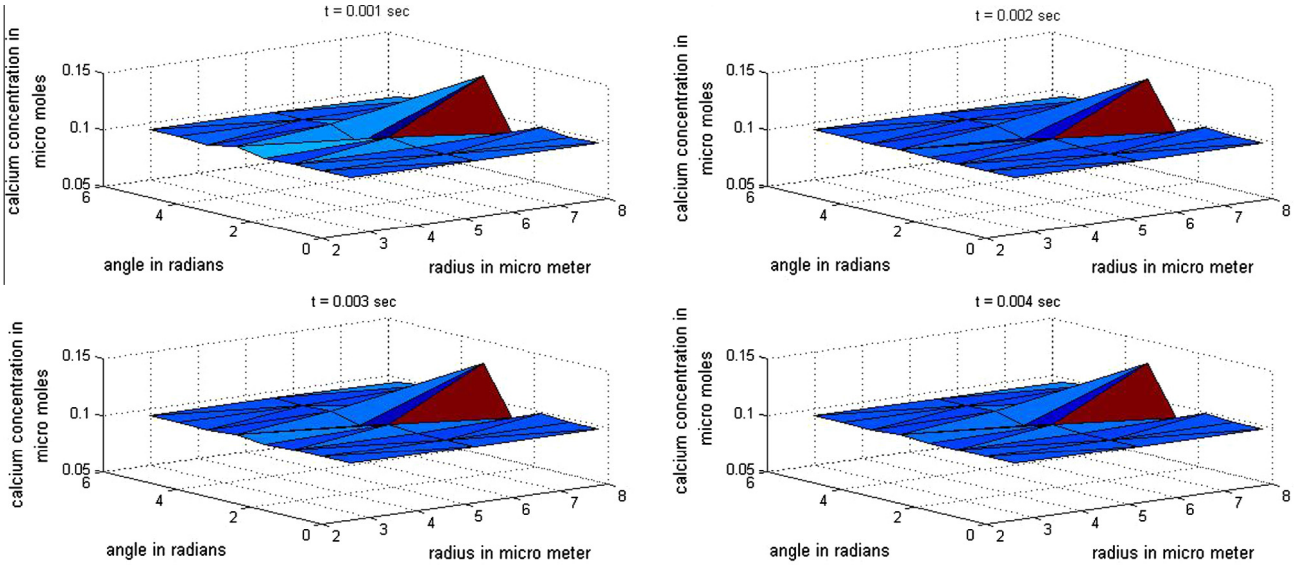

Figure 2 Spatiotemporal calcium distribution at time t = 0.001, 0.002, 0.003 and 0.004 s.

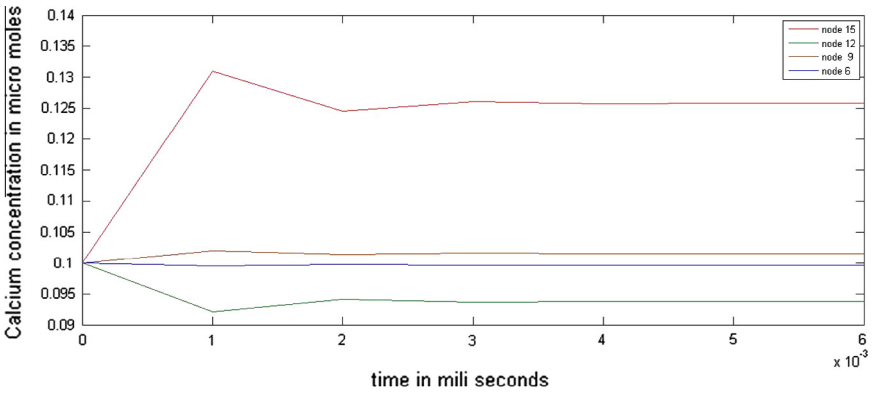

Figure 3 Spatiotemporal calcium distribution at different nodes 15, 12, 9 and 6.

3. Results and discussion

A computer program in MATLAB 7.10.0.4 is developed to find numerical solution to the entire problem. The time taken for simulation is nearly 8.81 s on Core (TM) i 5-520 M 330 @ 2.40 GHz processing speed and 4 GB memory. To find the solution of equation (3.2.10) the biophysical parameters are taken from the literature as shown in Table 2.

In Fig. 2(a)–(d) it is observed that the calcium concentration is maximum at the source and it decreases as moving away from the source along radial and angular directions. The changes in peak calcium concentration at source with respect to time and calcium concentration at nodes far away from the source along angular and radial directions are plotted in Fig. 3.

In Fig. 3 it can be seen that at the source (node 15: $r = 7.8$ μm, $\theta = \pi$), the calcium concentration increases from 0.1 to 0.131 μM in time $t = 0.001$ s. This elevation in calcium profile is due to the source influx. Then the calcium concentration is decreased to 0.1245 μM at the source at time $t = 0.002$ s. This is due to the buffering process. The buffer binds the calcium ion to reduce the free calcium concentration. Again some elevation in calcium concentration is observed at $t = 0.003$ s due to influx. This increase and decrease in calcium concentration at the source and other nodes (node 12: node 15: $r = 7.8$ μm, $\theta = 3\pi/4$, node 9: $r = 7.8$ μm, $\theta = \pi/2$, node 6: $r = 7.8$ μm, $\theta = \pi/4$) are observed up to 0.004 s and then thereafter the calcium concentration becomes stable and constant. Thus the system achieves steady state in 0.004 s. The variation in calcium concentration is highest at source and it decreases as moving away from the source. This variation in calcium concentration at the source is observed due to mismatch among influx, buffering and diffusion of calcium in the cell. When the system achieves coordination of these processes the system reaches it steady state.

Fig. 4 shows the spatiotemporal calcium concentrations for different source influxes 1 pA, 2 pA and 3 pA at time $t = 0.001$ s. It is observed that the calcium concentrations increase in ratio of source influx. It is also observed that the oscillation in concentration is also in the ratios to the source influx. For

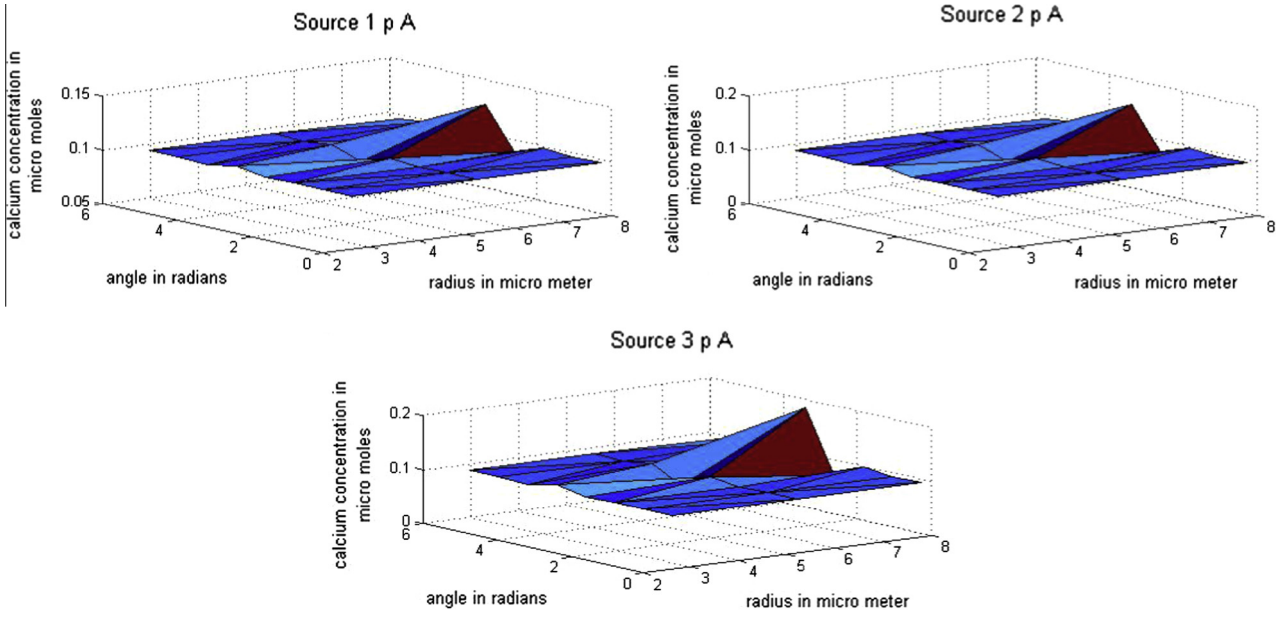

Figure 4 Spatiotemporal calcium distributions for influxes 1 pA, 2 pA and 3 pA.

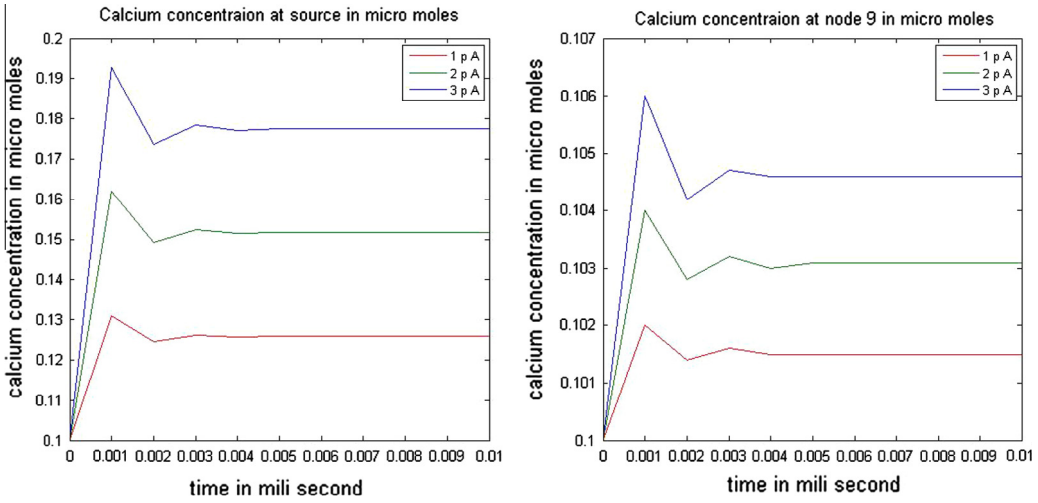

Figure 5 Spatiotemporal calcium distributions for different influxes at nodes (7.8, π) and (7.8, $\pi/2$).

high value of source influx the more oscillation is observed and it required more time to achieve steady state. The system achieves steady state condition in time $t = 0.005$, 0.006 and 0.008 s for influx 1 pA, 2 pA and 3 pA respectively.

Fig. 5 shows the calcium concentrations for different source influxes 1 pA, 2 pA and 3 pA at nodes (7.8, π) and (7.8, $\pi/2$). It is observed that variation of calcium concentration in the cell at source and other nodes is more at higher rates of source influx. The increase in calcium concentration at source and other nodes is in ratio of source influx. But for node (7.8, $\pi/2$) away from the source the oscillations are less than those at node (7.8, π). The variation in calcium concentration is highest at source and it decreases as moving away from the source. This variation in calcium concentration at the source is observed due to mismatch among influx, buffering and diffusion of calcium in the cell. This means that near the source effect of source influx is more as compared to that at nodes away from the source.

Fig. 6 shows the spatiotemporal calcium concentrations for different buffer concentrations 50 μM, 100 μM and 150 μM. It is observed that the calcium concentrations decrease in ratio of buffer concentrations. It is also observed that the oscillation in concentration is also in the ratio to the buffer concentrations. For high value of buffer concentration the more oscillations are observed. The system achieves steady state condition in time $t = 0.006$, 0.007 and 0.008 s for buffer concentrations of 50 μM, 100 μM and 150 μM respectively.

Fig. 7 shows the calcium concentrations for different buffer concentrations 50 μM, 100 μM and 150 μM at nodes (7.8, π) and (7.8, $\pi/2$). It is observed that oscillations increase in ratio of buffer concentrations for both the nodes (7.8, π) and (7.8, $\pi/2$). But for node (7.8, $\pi/2$) which is away from the source the oscillations are less as compared to those at node (7.8, π). Hence oscillations decrease as we moving away from the source. This means that near the source the effect of buffer is less compared to that at nodes away from the source.

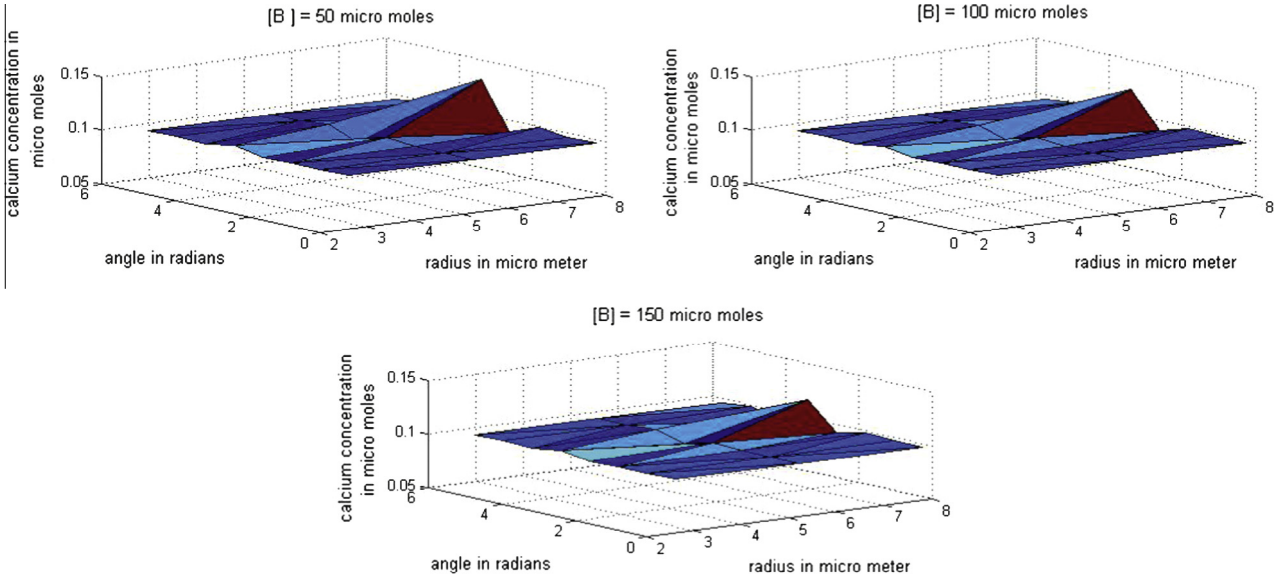

Figure 6 Spatiotemporal calcium distributions for different buffer concentrations.

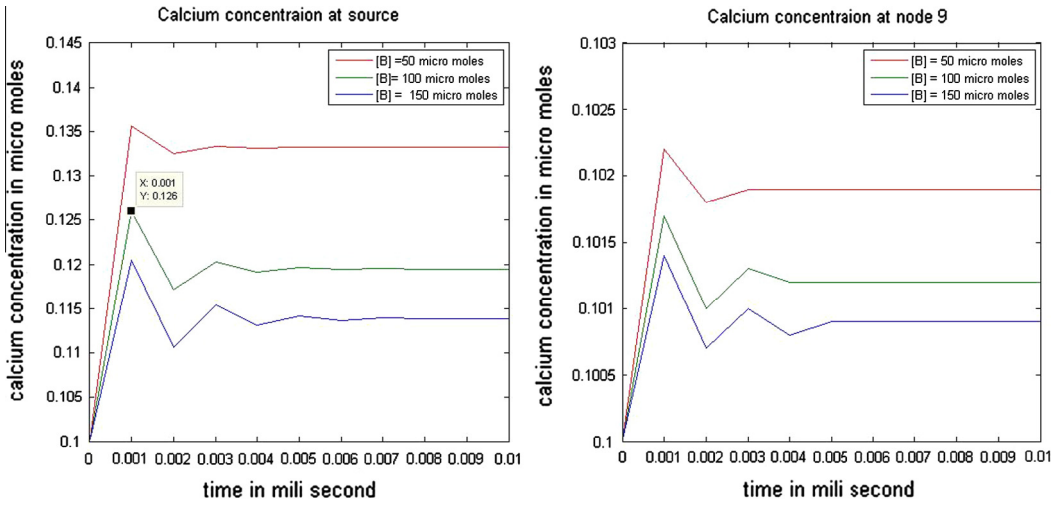

Figure 7 Spatiotemporal calcium distribution for different buffer concentrations at nodes.

4. Conclusions

A finite element model is proposed and employed to study two dimensional spatiotemporal calcium distributions in cardiac myocytes involving processes such as influx, buffering and diffusion. The model gives us interesting spatiotemporal calcium patterns in relation to the multiphysical processes in cell. On the basis of results it is concluded that the calcium concentration in the cell increases in ratio of source influx and decreases in the ratio of buffer concentration. In the initial period of time the physical processes such as influx and buffering cause oscillation in calcium concentration in the cell until the process reaches steady state. Thus cardiac myocytes exhibit a beautiful mechanism of well coordinated effect of multiphysical processes such as buffering, diffusion and influx for regulating the calcium concentration required for maintaining structure and function of the cell. The finite element approach is quite versatile in the present condition of the problem as it gives such flexibility to incorporate theses multiphysical processes in the model. Such models can be developed further for generating information of spatiotemporal calcium concentration patterns required for contraction and expansion of myocytes which is responsible for blood circulation in the human body. This information can be useful to biomedical scientist for developing protocols for diagnosis and treatment of diseases related to heart. In all it is contribution of new knowledge and new research progress in the field of computational cell biology.

Conflict of interest

The authors declare that there are no conflict of interests.

Acknowledgments

Authors are highly thankful to CSIR, New Delhi and DBT, New Delhi, for providing financial assistance and infrastructure facility at SVNIT, Surat, to carry out this research work.

References

1. Smith GD, Keizer JE, Stern MD, Lederer WJ, Cheng H. Simple numerical model of calcium spark formation and detection in cardiac myocytes. *Biophys J* 1998;**75**:15–32.
2. Michailova A, Del F, Egger M, Niggli E. Spatiotemporal features of Ca^{2+} buffering and diffusion in atria cardiac myocytes with inhibited sarcoplasmic reticulum. *Biophys J* 2002;**83**:3134–51.
3. Jha A, Adlakha N. Two dimensional finite element model to study unsteady sate calcium diffusion in neuron involving ER Leak and SERCA. *Int J Biomath* 2015;**8**(1):155000. http://dx.doi.org/10.1142/S1793524515500023, 14p.
4. Jha A, Adlakha N. Analytical solution of two dimensional unsteady state problem of calcium diffusion in a neuron cell. *J Med Imaging Health Inform* 2014;**4**(4):547–53.
5. Tripathi A, Adlakha N. Finite element model to study calcium diffusion in a neuron cell involving J_{RYR}, J_{SERCA} and J_{Leak}. *J Appl Math Inform* 2013;**3**:695–700.
6. Tripathi A, Adlakha N. Two dimensional coaxial circular elements in FEM to study the calcium diffusion in Neuron cells. *Appl Math Sci* 2012;**6**:455–66.
7. Jha BK, Adlakha N, Mehta MN. Two-dimensional finite element model to study calcium distribution in astrocytes in presence of excess buffers. *Int J Biomath* 2014;**7**(3):145003. http://dx.doi.org/10.1142/S1793524514500314, 11p.
8. Jha BK, Adlakha N, Mehta MN. Two-dimensional finite element model to study calcium distribution in astrocytes in presence of VGCC and excess buffers. *Int J Model Simul Sci Comput* 2013;**4**(2):1250030. http://dx.doi.org/10.1142/S1793962312500304, 15p.
9. Kotwani M, Adlakha N, Mehta MN. Finite element model to study the effect of buffers, source amplitude and source geometry on spatio-temporal calcium distribution in fibroblast cell. *J Med Imaging Health Inform* 2014;**4**(6):840–7.
10. Manhas N, Pardasani KR. Mathematical model to study IP3 dynamics dependent calcium oscillations in pancreatic acinar cells. *J Med Imaging Health Inform* 2014;**4**(6):874–80.
11. Manhas N, Pardasani KR. Modelling mechanism of calcium oscillations in pancreatic acinar cells. *J Bioenerg Biomembr* 2014;**46**(5):403–20.
12. Manhas N, Sneyd J, Pardasani KR. Modelling the transition from simple to complex Ca^{2+} oscillations in pancreatic acinar cells. *J Biosci* 2014;**23**(3):463–84.
13. Naik P, Pardasani KR. Finite element model to study calcium distribution in Oocytes involving voltage gated Ca^{2+} channel,

ryanodine receptor and buffers. *Alexandria J Med* 2016;**52**(1):43–9.
14. Naik P, Pardasani KR. One dimensional finite element model to study calcium distribution in oocytes in presence of VGCC, RyR and buffers. *J Med Imaging Health Inform* 2015;**5**(3):471–6.
15. Panday S, Pardasani KR. Finite element model to study effect of advection diffusion and Na^+/Ca^{2+} exchanger on Ca^{2+} distribution in Oocytes. *J Med Imaging Health Inform* 2013;**3**(3):374–9.
16. Panday S, Pardasani KR. Finite element model to study the mechanics of calcium regulation in oocytes. *J Mech Med Biol* 2014;**14**(2). http://dx.doi.org/10.1142/S0219519414500225.
17. Tewari S, Pardasani KR. Finite element model to study two dimensional unsteady state cytosolic calcium diffusion. *J Appl Math Inform* 2011;**29**:427–42.
18. Tewari S, Pardasani KR. Finite element model to study two dimensional unsteady state cytosolic calcium diffusion in presence of excess buffers. *IAENG J Appl Math* 2010;**40**(3):1–5.
19. Tewari S, Pardasani KR. Modelling effect of sodium pump on calcium oscillation in neuron cells. *J Multiscale Model* 2012;**4**(3):1250010. http://dx.doi.org/10.1142/S1756973712500102, 16p.
20. Backx PH, De Tonb PP, Jurjen K, Deen Van, Barbara JM, Henke DJ. A model of propagating calcium-induced calcium release mediated by calcium diffusion. *J Gen Physiol* 1989;**93**:963–77.
21. Shannon TR, Wang F, Puglisi J, Weber C, Bers DM. A mathematical treatment of integrated Ca dynamics within the ventricular myocytes. *Biophys J* 2004;**87**:3351–71.
22. Post J, Langer G. Sarcolemma Ca^{2+} binding sites in heart: I. Molecular origin in gas dissected. *J Membr Biol* 1992;129–49.
23. Luo, Rudy. A dynamic model of the cardiac ventricular action potential I simulations of ionic currents and concentration changes. *Circ Res* 1994;**74**:1071–96.
24. Luo, Rudy. A dynamic model of the cardiac ventricular action potential II. After depolarization triggered activity and potentiation. *Circ Res* 1994;**74**:1097–113.